ASPS Conference Proceedings 1: 835-841 (2022)

Proceedings of

12th Structural Engineering Convention-An International Event (SEC 2022)

Available at https://asps-journals.com/index.php/acp

# Behaviour of Intermediate Moment Resisting RC Frame Structures Under The Influence of P-Delta Effect

N. Samanta[1,*], K. Dasgupta[2], R. Khare[3]

[1]Department of Civil Engineering and Applied Mechanics, Post Graduate Student, Shri G.S. Institute of Technology & Science, Indore, 452003, India
[2]Department of Civil Engineering, Associate Professor, Indian Institute Technology, Guwahati, 781039, India
[3]Department of Civil Engineering and Applied Mechanics, Professor, Shri G.S. Institute of Technology & Science, Indore, 452003, India,

**Paper ID - 060379**

**Abstract**

Among the different categories of RC frames based on the implemented ductile detailing of the members, Intermediate Moment Resisting Frame (IMRF) is imparted with medium ductility capacity. Buildings with IMRF are intended to be used in Indian Seismic Zone III which refers to moderate level of seismic risk. Although past research has focused extensively on seismic behaviour of non-ductile and fully ductile moment resisting frames, very few studies on IMRF behaviour have been carried out. Also, the influence of *P*-Delta (*P*-Δ) effect on nonlinear behaviour of RC frame buildings has been studied to a limited extent. The present study aims to study the influence of imposed displacement pattern on the nonlinear behaviour of IMRF considering the *P*-Δ effect. Initially, single RC frame building five-storey with symmetrical floor plan, is designed as per the relevant Indian guidelines considering possible IMRF behaviour. Although the detailing of frames with medium ductility is absent in the current Indian Code IS: 13920-2016, the same has been carried out as per the draft IS: 13920. Displacement-controlled nonlinear static analysis or pushover analysis is carried out for the designed frames. For the distribution of imposed displacement pattern along the height of the frame, 4 different profiles are adopted, namely (a) parabolic as per IS: 1893 (Part 1) – 2016, (b) uniform, (c) fundamental mode shape and (d) triangular. It is found that under *P*-Δ effect, the initial lateral stiffness and base shear capacity get reduced for all the frames. The same can be correlated with the higher lateral displacement Thus, the absence of *P*-Δ effect causes overestimation of base shear capacity for the IMRF. The initial global stiffness predicted by the IS: 1893 (Part 1) – 2016 is the least among the lateral stiffness observed under all the load patterns. However, the uniform displacement profile provides the maximum base shear capacity of IMRF among all the load patterns.

*Keywords*: Intermediate Moment Resting RC frame (IMRF); P-DELTA effect; Different load patterns

## 1. Introduction

Philosophy of earthquake resistant design is primarily based on ductility capacity of a particular structure. In case of RC frame structures ductility is imparted through detailing of reinforcement. In Indian context, depending on the imparted ductile detailing, two categories of RC moment-resisting frames are constructed, namely (i) Ordinary Moment Resisting Frame (OMRF) based on guidelines of IS 456:2000 [1] and (ii) Special Moment Resisting Frame (SMRF) as per guidelines of IS 13920:2016 [2]. India has been divided into 4 seismic zones such as Zone II, Zone III, Zone IV and Zone V according to IS 1893 (Part1):2016 [3]. In Zone II, OMRF is mainly used (for Zone II SMRF is kept optional as per IS 13920) due to low ductility requirements, whereas for rest of seismic zones, SMRF is recommended for construction as per IS 13920. From extensive literature survey it has been found that various International Standards such as ASCE7:2016 [4], EC8:2004 [5], NZS1170.5:2004 [6] recommend three kinds of ductile detailing for earthquake resistant structures. These three kinds of ductile detailing indicate three levels of energy dissipative capacity of RC frame structures which can be adopted as per seismic hazard demand. ASCE7 stipulates three ductility classes such as ordinary Moment Resisting Frame (OMRF), Intermediate Moment Resisting Frame (IMRF) and Special Moment Resisting Frame (SMRF). Similarly EC8 classifies building as per ductility class such as low (DCL), medium (DCM) and high (DCH). On the other hand NZS 1170.5 classifies the frame structures based on their natural period, namely (i) long period (≥ 0.7sec) frames, and (ii) short period (< 0.7 sec) frames. For each category, structures have been further classified into three ductility classes such as Ductile Structures (DS), Structures of Limited Ductility (SLD) and Nominal Ductile Structures (NDS)

In India, seismic hazard in terms of peak ground acceleration (PGA) for Zone IV and Zone V is 1.5 times and 2.25 times higher as compared to Zone III. To make ductile detailing practice rational, draft IS 13920 [7] (based on IITGN-World Bank Project on Seismic Codes) has adopted the provision of Intermediate Moment Resisting Frame (IMRF) for seismic zone III. Allahyari et al. [8] evaluated the performance of special and intermediate moment resisting RC frames using pushover analysis and

*Corresponding author. Tel: +916265199893; E-mail address: nilanjan.civil@gmail.com



Published online: December 19, 2022
doi:10.38208/acp.v1.591

incremental dynamic analysis. Lu et al. [9] did experimental investigation of 3 RC frames having 3 levels of ductility capacity and concluded that the seismic performance of medium ductile frame (DCM) is superior as compared to high ductile frame (DCH). Moss and Carr [10] studied the influence of *P*-Delta, (*P*-Δ) effect on the behaviour of tall concrete frames. From literature survey, it has been found that past research has focused extensively on seismic behaviour of non-ductile and fully ductile moment resisting frames in Indian context, but very few studies on behaviour of IMRF have been carried out. Also, the influence of *P*-Δ effect on nonlinear behaviour of IMRF buildings has been studied to a limited extent.

## 2. General Features of IMRF

IMRF is basically a medium ductile structure intended to be used for moderate seismic zones. The draft IS 13920 [7] stipulates certain ductile detailing provisions for IMRF (RC) structures, with the salient features shown in Table 1.

## 3. Effect of P-Delta on Nonlinear Response

A conceptual description of *P*-Δ effect on inelastic behaviour of RC member can be depicted by considering backbone curve of a SDOF system. For sake of simplicity nonlinear behaviour of RC member can be assumed to be bilinear along with zero post-yield stiffness. Fig 1(a) shows a cantilever having height $H$ and supporting a single mass $M$. Gravity load $P$ is acting downwards and equivalent lateral force $F_o$ is acting horizontally at the top of the cantilever. Due to the effect of lateral force $F_o$ (equal to base shear strength $V_B$), the resulting displacement Δ leads to a secondary moment *P*-Δ and an overturning moment $F_o.H$. The secondary moment and overturning moment together constitute the overturning capacity $M_{OT}$. Figure 1(b) shows without *P*-Δ effect lateral force level is $F_o$ with initial stiffness $K_o$. With inclusion of *P*-Δ effect, these quantities are reduced to $F_p$ and $K_p$.

Table-1. Salient Features of IMRF

| Detailing pertaining to | Recommendation of Draft IS 13920 |
|---|---|
| Flexure members- longitudinal reinforcements | 1) Positive steel at any joint face equal to 1/3 of negative steel at that face<br>2) Steel provided at any face at any section shall be at least 1/5 of maximum negative steel at any joint face |
| Shear capacity of web reinforcement | Shear required for design gravity load + Shear developed by sum of moment resistance of both ends of member |
| Column lap splices | Maximum 50 percent rebars can be lapped in one location |
| Shear capacity of transverse reinforcement in columns | Shear developed by sum of moment capacity of both ends of member |
| Strong Column and Weak Beam | Not considered |

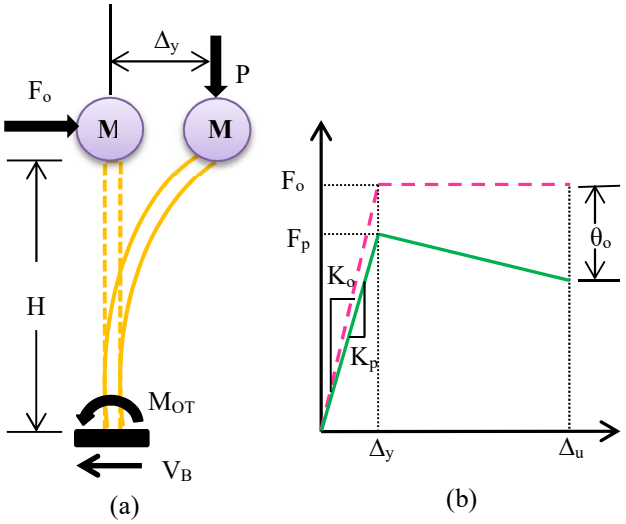


Fig. 1. P-Delta effect on RC column

At the onset of yield displacement $\Delta_y$, lateral force $F_p$ can be correlated to $F_o$ by the standard form [11] as

$$F_p = F_o - \frac{P\Delta_y}{H}. \quad (1)$$

By using stability ratio ($\theta_o$), Eq. (1) can be further simplified as,

$$\theta_o = \frac{P\Delta_y}{F_o H} = \frac{P}{K_o H} \quad (2)$$

$$F_p = F_o - \theta_o K_o \Delta_y = F_o(1-\theta_o) \quad (3)$$

$$K_p = K_o(1-\theta_o) \quad (4)$$

## 4. Description of Structural System Adopted

A five-storied RC frame building having symmetric plan is considered in the present study (Figs. 2 and 3). The building configuration is intended to represent regular residential building in seismic zone III as per IS: 1893 (Part 1) [3]. Accordingly, the design level seismic demand for this building is obtained in terms of design base shear as per equivalent static method. As the building height is more than 15 m, therefore design base shear obtained by equivalent static method is further compared with the value obtained using response spectrum method. For computation of design base shear, zone factor ($Z$) is taken as 0.16, importance factor ($I$) is taken as 1. Response reduction factor ($R$) value is given on IS 1893 (Part 1) [3] for SMRF as 5 and for OMRF as 3. The draft IS 1893 [12] had proposed $R$ value for IMRF (intended to be medium ductile frame) as 4 which is adopted in the present study. Spectral acceleration is considered for rocky soil site without any soil-structure interaction as per the guideline of IS 1893 (Part 1) [3]. Grade of concrete is taken as M25 and grade of reinforcement bar is taken as Fe 415. Fig. 4 shows reinforcement details of beam and column sections at the end of members of the adopted IMRF.

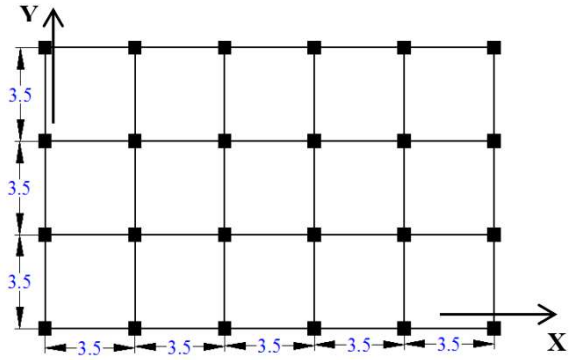


Fig. 2. Typical plan of adopted buildings
(All dimensions are in metre)

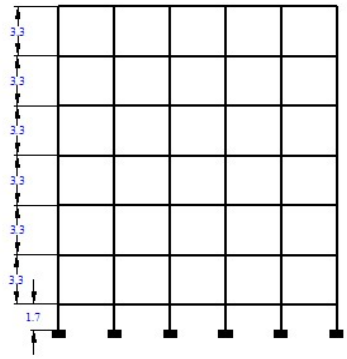


Fig. 3. Typical elevation of typical five-storey IMRF (All dimensions are in metre)

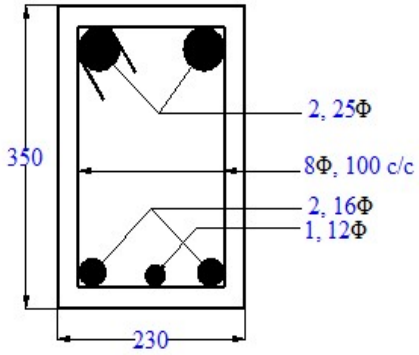


(a)

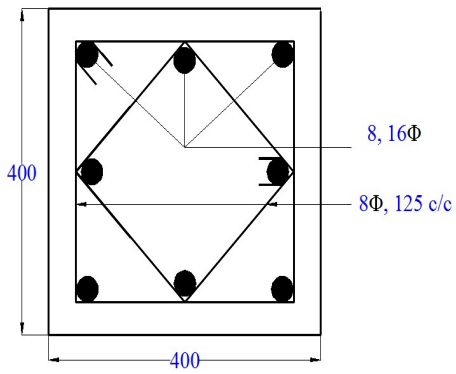


(b)

Fig. 4 Reinforcement details for (a) beam and (b) column sections in the five-storey IMRF building
(All dimensions are in millimetre)

## 5. Modelling of IMRF Members

Modelling of considered IMRF is done on SAP2000 V19 [13]. All buildings are modelled as space frames and rigid diaphragm is assigned to all the floors except the ground floor. Joint panels are considered to be rigid and it is assumed that joints are sufficiently strong to avoid any premature failure before occurrence of mechanism in other members. To consider cracked stiffness of the RC sections, 35% of gross moment of inertia is considered for the beams and 70% of gross moment of inertia is considered for the beams [3]. Component level nonlinear behaviour of IMRF members primarily depends on moment-rotation property which directly depends on two factors, namely (a) moment-curvature behaviour of plastic hinge section and (b) plastic hinge length.

### *5.1. Moment-Curvature Behaviour of RC Sections*

Moment-curvature characteristics ($M$-$\phi$) of RC sections are implemented by using well accepted Mander et al. [14] model. Draft IS 13920 indicates that close transverse reinforcements at RC member ends should be capable to confine concrete core. To take into account, Mander confined concrete has been assigned to concrete within stirrups and Mander unconfined concrete has been assigned to cover concrete to simulate realistic condition of frame section. Spalling of concrete cover is simulated as the strain outside the confinement area or core exceeds peak strain (under compression) of unconfined concrete. In this study ultimate compressive strain of unconfined concrete is taken as 0.005 according to Priestley [15]. Ultimate compressive strain of confined concrete is taken 0.02 according to ATC 40 [16] as this limit prevents bucking of longitudinal rebar in between consecutive transverse stirrups. Due to the presence of rigid floor diaphragms, the effect of axial load on $M$-$\phi$ characteristics of beams is neglected. Fig. 5 shows typical $M$-$\phi$ curve of beam section of five-storey IMRF building for both hogging (top tension) moment and sagging (bottom tension) moment. Similarly Fig. 6 shows typical $M$-$\phi$ curve of column section of five-storey IMRF building for different amount of axial load ($P_u$) normalized to its axial load capacity ($P_{uz}$). It is found that for each $M$-$\phi$ curve, there is a drop in the curve after reaching maximum moment capacity which occurs due to spalling of cover concrete. This phenomenon is more prominent in column sections with increasing axial load level.

### *5.2. Plastic hinge characteristics of RC sections*

Plastic rotation capacity ($\theta_p$) of a typical RC section depends on ultimate curvature ($\phi_u$), yield curvature ($\phi_y$) and plastic hinge length ($L_p$). This can be expressed by simple form as-

$$\theta_p = (\emptyset_u - \emptyset_y).L_p \quad (4)$$

Lots of researchers have proposed various expressions for estimation of plastic hinge length [17-19]. In this study, the formulation given by Park and Paulay [17] has taken into consideration. Experiments conducted by Basha and Kaushik [20] indicate that the expression of Park and Paulay

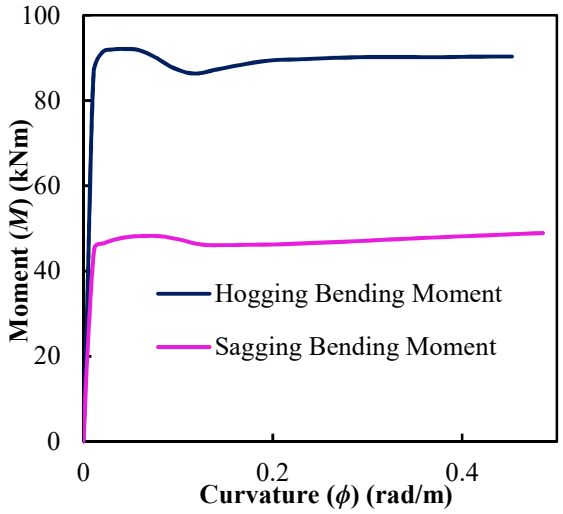


Fig. 5. Sample $M$-$\phi$ curve of beam section of five-storey IMRF building

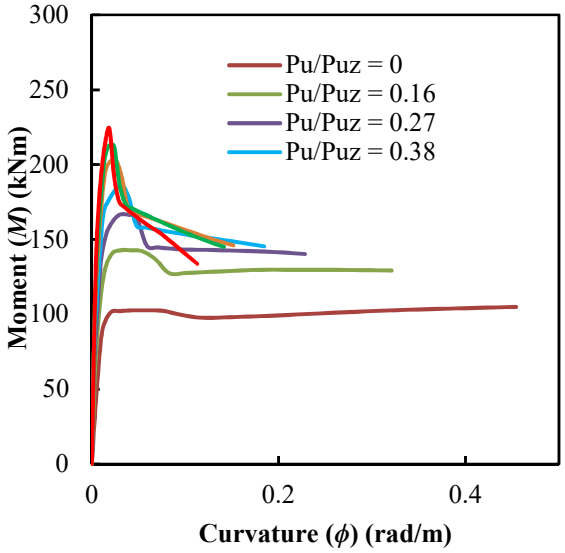


Fig. 6. Sample $M$-$\phi$ curve of column section of five-storey IMRF building

closely matches with experimental results. Equation of Park and Paulay can be expressed as,

$$L_p = 0.5H, \tag{5}$$

where, $L_p$ is the length of plastic hinge and H is the depth of section.

*5.3. Plastic hinge details*

In this study lumped plastic hinge model is adopted. As certain relaxation in ductile detailing has been adopted in case of IMRF, as compared to SMRF, there remains a possibility of shear failure in IMRF members prior to flexure failure. To investigate this phenomenon, force controlled shear hinge is adopted. Modelling of shear hinges is done by using the following expressions:

$$V_u = V_c + V_s \tag{6}$$

$$\text{For beams, } V_c = \tau_c bd \tag{7}$$

$$\text{For columns, } V_c = \delta\tau_c bd \tag{8}$$

For both columns and the beams,

$$V_s = \frac{f_y A_{sv} d}{s_v}, \tag{9}$$

where $V_u$ s the shear capacity of RC members, $V_c$ represents shear capacity of concrete sections, $V_s$ represents shear capacity of steel. $\tau_c$ is design shear strength of concrete, and $\delta$ is shear strength enhancement factor (according to IS456:2000). Here $f_y$ is the yield stress of transverse reinforcement, $A_{sv}$ is the total cross sectional area of one stirrup considering all legs, $d$ is the effective depth and $s_v$ is Spacing between two stirrups.

On the other hand, for flexure failure, deformation controlled flexural hinge is used for this study according to $M$-$\phi$ relationship of sections. For beam, hinges (M3 and V2) have been assigned at a distance $L_p/2$ from face of the beams. In similar way for column coupled axial-moment (P-M2-M3) hinges and shear (V2 and V3) hinges have been inserted at column at a distance $L_p/2$ from face of the columns. Fig 7 shows typical P-M2-M3 interaction employed in this study.

## 6. Nonlinear Static (Pushover) analysis of IMRF

Nonlinear static or pushover analyses have been performed in this study for the adopted IMRF buildings along both X and Y directions. Pushover analyses comprise of two stages, namely (i) application of gravity load under force controlled manner, and (ii) subsequent application of lateral force under displacement controlled manner. This invariant lateral force distribution along storey height represents likely distribution of inertia forces induced on frame during a seismic excitation. As no single lateral load distribution can detect variation of local demands expected in a seismic excitation, various International Standards [16, 21] advocates minimum 2 lateral load patterns to overcome this problem. In this study, 4 load patterns have been employed that can represent likely distribution of inertia force. These lateral load patterns are-

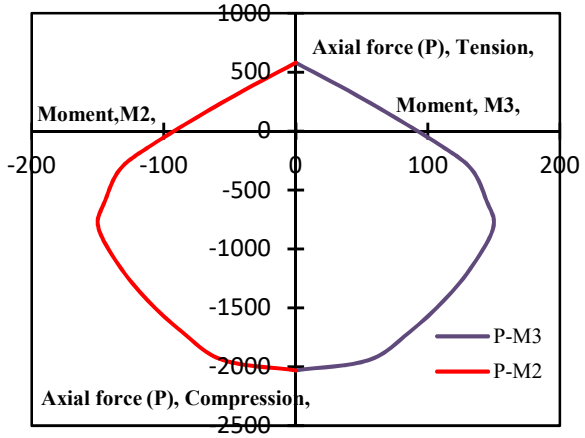


Fig. 7. Typical P-M2-M3 interaction of five-storey IMRF

a) Uniform distribution
b) Fundamental Mode proportional
c) Triangular distribution
d) IS 1893-Parabolic distribution

As lateral pushover analysis is displacement controlled procedure, therefore these load patterns are representative of the imposed displacement pattern distributed along the building height. In this study, the effect of geometric nonlinearity on IMRF is taken by *P*-Δ effect. For both Push X and Push Y, inclusion and exclusion of *P*-Δ effect are envisaged. In pushover analyses, the behaviour of the structure is depicted by capacity curve which represents the variation of base shear with roof displacement.

## 7. Results of Pushover analyses

After performing pushover analyses, capacity curve for IMRF building is obtained along X and Y directions. Capacity curves along both directions show that peak strength is maximum without P-Delta effect as compared to the value considering P-Delta effect.

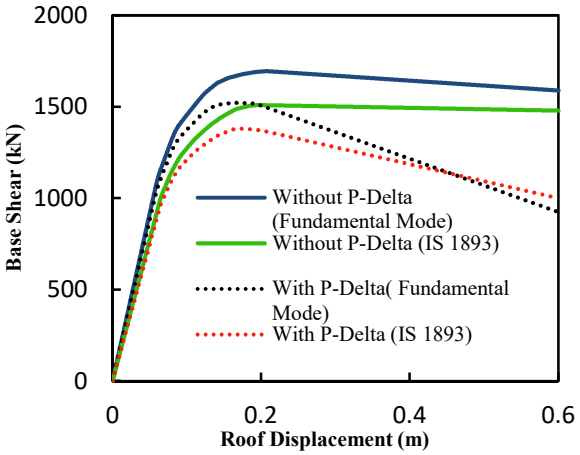


Fig. 8. Capacity curve along X direction of five-storey IMRF

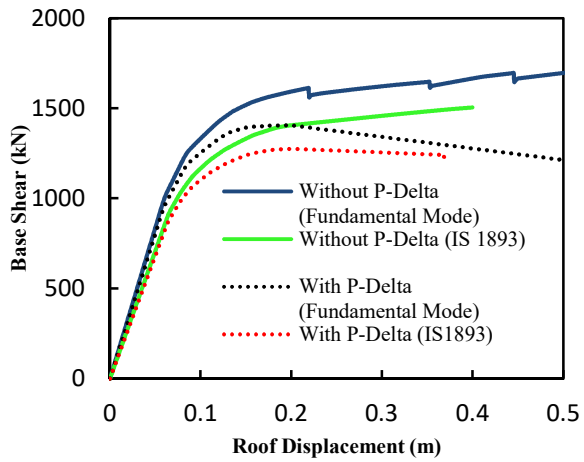


Fig. 9. Capacity curve along Y direction of five-storey IMRF

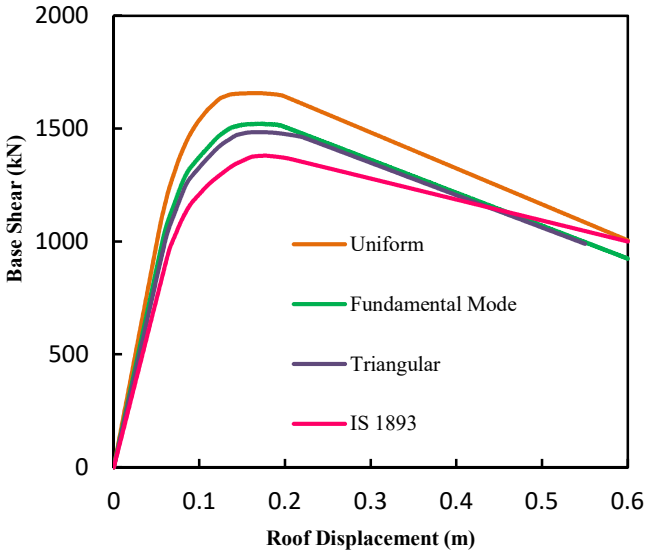


Fig. 10. Capacity curve along X direction of five-storey IMRF under P-Delta effect

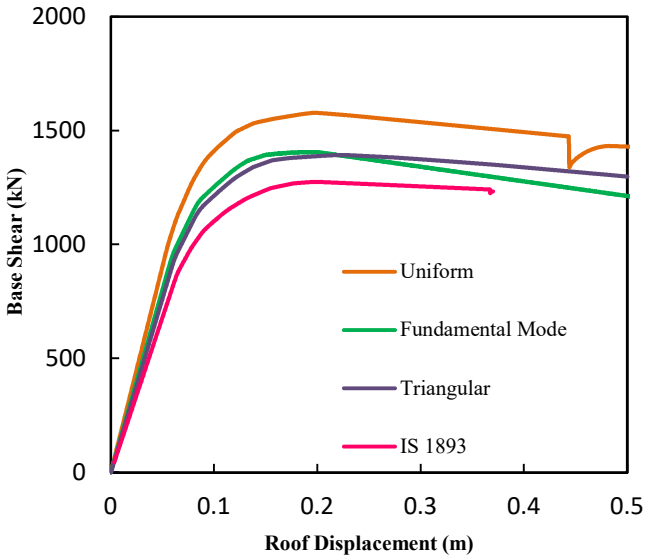


Fig. 11. Capacity curve along Y direction of five-storey IMRF under P-Delta effect

Figs. 8 and Fig. 9 show that for both X and Y directions without *P*-Δ effect, post yield behaviour of capacity curve either decreases monotonically at a mild slope or increases monotonically. Capacity curve along Y direction under mode proportional load, indicates degraded saw-tooth type of curve. This is observed due to the fact that as software finds any degraded element on model, it revises the model to reflect the degraded element on the model and rebuilds new capacity curve. It has been found that for the capacity curve along X direction (Fig. 8), the peak strength reduces approximately in between 8-10 percent considering *P*-Δ effect. For capacity curve along Y direction (Fig. 9), the peak strength in terms of base shear capacity sharply reduces approximately in the range of 18% - 28% due to *P*-

Δ effect. For capacity curve along X direction, it is also found out that the effective stiffness reduces 3.5% - 4% approximately. In case of capacity curve along Y direction, the effective stiffness decreases in the range of 2.5% - 3%. From Figs. 8 and 9, it is also evident that the displacement ductility under *P*-Δ effect reduces rapidly as compared to the ductility obtained without *P*-Δ effect.

Figs. 10 and 11 show the influence of various lateral displacement patterns on IMRF frame in the presence of *P*-Δ effect. It is found out that the uniform lateral displacement pattern yields highest value of base shear capacity among various displacement patterns considered, whereas IS 1893 displacement pattern (parabolic pattern) shows the lowest value of base shear capacity. Fundamental mode proportional displacement pattern and triangular displacement pattern give nearly equal base shear capacities and displacement ductilities. Therefore from the point of view of maximum base shear capacity, uniform distribution gives the upper bound value, whereas IS 1893 (Part 1):2016 pattern yields the lower bound value. Other considered displacement pattern gives intermediate results. These various types of adopted displacement patterns represent inertia force distribution of building. It is also evident that the initial stiffness for the IS 1893 displacement pattern is lower for both X and Y directions as compared to other displacement patterns. This is quite expected for the same level of base shear, as storey forces at upper levels are larger for IS 1893 displacement pattern as compared to the other adopted displacement patterns which naturally result in larger elastic roof displacement.

## Disclosures

Free Access to this article is sponsored by SARL ALPHA CRISTO INDUSTRIAL.

## 8. Conclusions

From the present study, the following are the salient conclusions:

1) *P*-Δ effect is an important part of geometric nonlinearity which must be taken into account for IMRF as it has strong influence on building base shear capacity and displacement ductility.
2) Without *P*-Δ effect, the capacity curves either increase monotonically or get reduced at a mild slope in the post-yield phase.
3) Under *P*-Δ effect, post yield stiffness reduces rapidly which significantly impairs displacement ductility.
4) It is evident that under *P*-Δ effect, IS 1893 (Part 1) load pattern gives conservative value of base shear capacity of buildings, whereas uniform load pattern gives upper bound value of base shear capacity.
5) Mode proportional load and triangular load patterns yield intermediate values of base shear capacity.
6) As *P*-Δ effect significantly reduces the initial stiffness and the base shear capacity of the buildings, there is a necessity to develop a new design methodology that incorporates design shear force in such a manner for which considering and ignoring *P*-Δ effect should be same.

## References

1. BIS, IS456. Plain and Reinforced Concrete – Code of Practice, Bureau of Indian Standards, New Delhi, India, 2000.
2. BIS, IS13920. Ductile Detailing of Reinforced Concrete Structures Subjected to Seismic Forces – Code of Practice, Bureau of Indian Standards, New Delhi, India, 2016.
3. BIS, IS1893. Criteria for Earthquake Resistant Design of Structures, Part 1, Bureau of Indian Standards, New Delhi, India, 2016.
4. ASCE, SEI/ASCE7-16. Minimum Design Loads for Buildings and Other Structures, American Society of Civil Engineers, Reston, USA, 2016.
5. CEN, Eurocode8. Design Provisions for Earthquake Resistance of Structures (European Prestandard ENV 1998), Comit´e Europ´een de Normalisation, Brussels, Belgium, 2004.
6. Standard, N. Z. and NZS1170.5. Structural design actions Part 5: Earthquake actions - New Zealand, Standard New Zealand, Wellington 6020, 2004.
7. Jain SK, Brzev S, and Rai DC. Proposed Modifications and Commentary for Code on Ductile Detailing of Reinforced Concrete Structures Subjected to Seismic Forces – Code of Practice (IS 13920:2016). IITGN-World Bank Project on Seismic Codes, EQ4-V1.0 & EQ5-V1.0 IIT, Gandhinagar, India, 2019.
8. Allahyari H, Keramati A, and Behbahani AAT. Performance evaluation of special and intermediate moment-resisting reinforced concrete frames using pushover and incremental dynamic analysis. The Structural Design of Tall and Special Buildings, 2011: 22(7): 584–592.
9. Lu Y, Hao H, Carydis PG, and Mouzakis H. Seismic performance of RC frames designed for three different ductility levels. Engineering structures, 2001; 23(5): 537-547
10. Moss PJ, Carr AJ. The effects of large displacements on the earthquake response of tall concrete frame structures. Bulletin of the New Zealand National Society for Earthquake Engineering, 1980; 13(4).
11. Silva PF, Sangtarashha A, and Burgueño R. P-Delta effects in limit state design of slender RC bridge columns. In 15th WCEE World Conference on Earthquake Engineering, Lisbon, Portugal, 2012.
12. Jain SK, Murty CVR. Proposed draft provisions and commentary on Indian seismic code IS 1893 (Part 1). IITK-GSDMA Project on Building Codes, EQ5-V4.0 & EQ15-V3.0 IIT, Kanpur, India, 2005.
13. CSI. Structural Analysis Program SAP2000 V19.0, Computers & Structures Inc., Berkeley, USA, 2018.
14. Mander JB, Priestley MJ, and Park R. Theoretical stress-strain model for confined concrete. Journal of Structural Engineering, ASCE, 1988; 114(8): 1804-1826.

15. Priestley MJN (1997). Displacement-based seismic assessment of reinforced concrete buildings. Journal of Earthquake Engineering, 1997; 1(01): 157-192.

16. ATC, ATC-40.Seismic Evaluation and Retrofit of Concrete Buildings. Volume 1, Applied Technology Council, Redwood City, USA, 1996.

17. Park R, Paulay T. Reinforced Concrete Structure. John Wiley & Sons, 1975.

18. Priestley MN, Seible F, and Calvi GM. Seismic design and retrofit of bridges. John Wiley & Sons, 1996.

19. Fardis MN, Biskinis DE. Deformation capacity of RC members, as controlled by flexure or shear. In Otani Symposium, 2003; Vol. 511530.

20. Basha SH, Kaushik HB. A novel macro model for prediction of shear failure in columns of masonry infilled RC frames under earthquake loading. Bulletin of Earthquake Engineering, 2019; 17(4): 2219-2244.

21. FEMA, FEMA-356.Prestandard and commentary for the seismic rehabilitation of buildings. Federal Emergency Management Agency, Washington (D.C.), USA, 2000.